Journal of the European Ceramic Society **9** (1992) 143–152

Micromechanical Stresses in Sapphire Whisker and Alumina Fiber Reinforced Mullite and Garnet Ceramic Matrix Composites*

Zhuang Li

Materials Science Division, Argonne National Laboratory, Argonne, Illinois 60439, USA

&

Richard C. Bradt

Mackay School of Mines, University of Nevada-Reno, Reno, Nevada 89557-0136, USA

(Received 17 May 1991; revised version received 4 July 1991; accepted 22 July 1991)

Abstract

Using a modified Eshelby approach which incorporates the thermoelastic anisotropy, the internal micromechanical residual stresses are calculated for both A-type and C-type single crystal sapphire whiskers reinforcing mullite and garnet polycrystalline ceramic matrix composites. Stresses for polycrystalline alumina reinforcing fibers were also determined. The residual stress levels for the whiskers are in the GPa range for the mullite matrix composite, where the sapphire whiskers have been reported to fracture. For the polycrystalline garnet matrix, the sapphire whisker anisotropy is highly influential on the residual stresses as the CTE of garnet is intermediate to the principal axial thermal expansion coefficients of sapphire. Residual stresses in polycrystalline alumina fibers in the same ceramic matrices are intermediate to the two orientations of the sapphire whiskers. The effects of externally applied loads are also investigated and are demonstrated to be carried primarily by the higher elastic modulus alumina components of the composites.

Für A-Typ und C-Typ Whisker aus Saphireinkristallen, die zur Verstärkung von Mullit- und polykristallinen Granat-Basiswerkstoffen eingesetzt wurden, konnten die internen mikromechanischen Restspannungen berechnet werden. Dazu wurde ein modifiziertes Verfahren nach Eshelby verwendet, das die thermoelastische Anisotropie mitberücksichtigt. Für die selben Basiswerkstoffe wurden ebenso die Spannungen für polykristalline Al_2O_3-Fasern bestimmt. Die auf die Whisker wirkenden Restspannungen liegen beim Mullit-Basiswerkstoff im GPa-Bereich, denen, nach Literaturangaben, die Saphirwhisker nicht standhalten. Für die Restspannungen im polykristallinen Granat-Werkstoff ist die Anisotropie der Saphirwhisker entscheidend, da der thermische Ausdehnungskoeffizient des Granats zwischen den beiden Werten der Saphirwhisker liegt. Die Restspannungen der mit polykristallinen Al_2O_3-Fasern verstärkten Basiswerkstoffe liegen zwischen den Werten, die sich für die beiden Saphirwhisker-orientierungen ergeben. Auf den Einfluß einer zusätzlichen äußeren Last wird ebenfalls eingegangen. Es hat sich gezeigt, daß diese hauptsächlich durch die Al_2O_3-Phase, die gegenüber der Matrix den höheren E-Modul aufweist, übernommen wird.

Par une approche Eshelby modifiée, incluant l'anisotropie thermoélastique, on a calculé les contraintes micromécaniques internes résiduelles pour des whiskers de saphir monocristallin type A et type C, renforçant des composites à matrice céramique polycristalline mullite et grenat. On a également déterminé ces mêmes contraintes pour des whiskers en fibres polycristallines d'alumine. Les niveaux de contraintes résiduelles pour les whiskers sont de l'ordre du GPa pour le composite à matrice mullite, dont les whiskers en saphir se fracturent. Pour la matrice grenat polycristallin, l'anisotropie du whisker

* Portions of this research were supported by NASA Grant No. NAGW-199 and by DOE, Basic Energy Sciences–Materials Sciences under Contract #W-31-109-ENG-38.

Journal of the European Ceramic Society 0955-2219/92/$5.00

saphir influe beaucoup sur les contraintes résiduelles, car le CET du grenat est intermédiaire entre les principaux coefficients axiaux d'expansion thermique de saphir. Les contraintes résiduelles dans les fibres polycristallines d'alumine, dans les mêmes matrices céramiques, sont comprises entre les valeurs obtenues pour les deux orientations des whiskers saphir. On a également étudié l'effet de charges extérieures appliquées et montré qu'il était principalement supporté par la fraction alumine du composite à module élastique élevé.

1 Introduction

Recently, there has been increased interest in the strengthening and the toughening of ceramic matrix composites that consist of the incorporation of single crystal ceramic whiskers within a polycrystalline ceramic matrix. One successful whisker for reinforcement has been SiC because it has one of the highest combinations of Young's modulus and strength. SiC whisker reinforced polycrystalline alumina matrix composites have been demonstrated to exhibit enhanced mechanical properties.[1-3] Other polycrystalline ceramics that have also been reinforced with SiC whiskers are silicon nitride and mullite matrices.[4-7] Another common ceramic that is commercially available in single crystal whisker form is sapphire or alumina. Sapphire also appears to have considerable potential as a ceramic composite reinforcing component for it has a high elastic modulus and can exhibit high strengths. In addition, as it is an oxide, sapphire resists oxidation at high temperatures and thus appears to be an excellent candidate for the reinforcing phase of several oxide matrices. The sapphire whisker–mullite matrix system has been considered particularly promising for it appears to be a thermodynamically stable one.[8] Recently, α-alumina fibers and whiskers have been utilized to reinforce mullite and yttrium–aluminum–garnet ($Y_3Al_5O_{12}$) matrix composites by Mah *et al.*[9] Although their results are interesting, they pose questions for both composite systems.

Research on ceramic whisker reinforced polycrystalline ceramic matrix composites has often emphasized the interfacial properties between the whiskers and the matrix. However, recent studies have demonstrated that the micromechanical internal residual stresses which are generated by the thermal expansion and elastic moduli differences between the reinforcing phase and the matrix also assume a very important role in the mechanical properties.[10-15] The micromechanical residual stresses within the aforementioned SiC whisker reinforced polycrystalline ceramic matrix composites have been calculated through the application of the Eshelby method by Li and Bradt.[15] Several researchers have experimentally measured the residual stresses, substantiating those theoretical calculations. However, the stresses which develop within sapphire whisker reinforced ceramic matrix composites have not been similarly considered, either theoretically or experimentally. This paper reports micromechanical stress calculations for single crystal sapphire whiskers and also for polycrystalline alumina fiber reinforced polycrystalline ceramic matrix composites with mullite and garnet ceramic matrices. The influence of the resulting stresses on the composite mechanical properties are also considered, confirming the likelihood of the fracture of sapphire whiskers in the mullite matrix as has been reported by Mah *et al.*[9]

2 Thermoelastic Properties and Formulation of Stress Calculations

Al_2O_3 as a reinforcing phase suitable for incorporation into ceramic matrix composites is commercially available in at least three common forms. One is a fine grain size polycrystalline alumina fiber and the other two are the A-type and the C-type orientations of single crystal sapphire whiskers. The A-type sapphire whisker has an axial orientation of $\langle 2\bar{1}\bar{1}0\rangle$ while the C-type whisker parallels the $\langle 0001\rangle$ direction. The principal axial thermal expansion coefficients and elastic properties of single crystal alumina have been experimentally determined[16,17] and have been discussed in detail by Salem *et al.*[18] They are listed in Table 1. The thermoelastic properties of single crystal sapphire whiskers are highly anisotropic, while those of polycrystalline alumina fibers can be assumed to be isotropic for the purposes of calculations, although some preferred orientation will inevitably be present in these fibers, depending upon their specific processing conditions.

The Young's moduli along the growth directions are high and similar for both A-type (430 GPa) and C-type (465 GPa) sapphire whiskers. This implies that the transverse elastic moduli of both types of whiskers are also similar for the $\langle 2\bar{1}\bar{1}0\rangle$ direction is perpendicular to the $\langle 0001\rangle$ direction. In contrast, the room temperature to 1000°C average thermal expansion coefficient parallel to the length of the C-type whisker, $\alpha_{\langle 0001\rangle}$, is $9{\cdot}15 \times 10^{-6}$/°C, more than 10% higher than that of the A-type whisker, $\alpha_{\langle 2\bar{1}\bar{1}0\rangle}$, which is only about $7{\cdot}94 \times 10^{-6}$/°C. Those values

Table 1. Thermoelastic properties of mullite, garnet and alumina[16-21a]

	Single crystals									
	C_{11}	C_{33}	C_{12}	C_{13}	C_{44}	C_{14}	$E_{\langle 0001\rangle}$	$E_{\langle 2\bar{1}\bar{1}0\rangle}$	α_{11}	α_{33}
Sapphire[16-18]	497	499	164	112	147	−23·6	465	430	7·94	9·15
	Polycrystalline materials									
	E	G	ν	α						
Alumina fiber[16-18]	402	169	0·23	8·34						
Mullite matrix[19]	220	87·0	0·27	5·60						
Garnet matrix[20,21]	283	110	0·25	8·90						

[a] E, G and C_{ij} are in GPa and α is in $\times 10^{-6}/°C$.

are also the principal axial thermal expansion coefficients of single crystal alumina, α_{33} and α_{11}, respectively. The transverse thermal expansion of the C-type whisker is isotropic and equal to α_{11}; however, that of the A-type whisker is anisotropic with a maximum value of α_{33} along the $\langle 0001\rangle$ and minimum value of α_{11} along the $\langle 10\bar{1}0\rangle$. For the purpose of the comparative calculations in this paper, the Young's modulus and the thermal expansion coefficient of the polycrystalline alumina fiber are both assumed to be the isotropic averages of the single crystal values and equal to 400 GPa and $8{\cdot}34 \times 10^{-6}/°C$, respectively. It was decided to use these average values since the various commercially available polycrystalline alumina fibers are all slightly different with respect to their texture development.

Table 1 also lists the thermal expansion and elastic moduli for the polycrystalline mullite and garnet matrices.[19-21] The Young's modulus of garnet is only slightly higher than that of mullite, but the Young's moduli for these two matrix materials are only about half the elastic modulus for alumina. The average thermal expansion of the two ceramic matrices from room temperature to 1000°C are quite different. Mullite is less than that of alumina, only about $5{\cdot}6 \times 10^{-6}/°C$, while garnet is about $8{\cdot}9 \times 10^{-6}/°C$, actually intermediate to the $\alpha_{\langle 0001\rangle}$ and $\alpha_{\langle 2\bar{1}\bar{1}0\rangle}$ thermal expansion coefficients of single crystal sapphire. These subtle differences significantly affect the magnitudes and distributions of the internal micromechanical residual stresses that result from cooling during processing and may also be expected to significantly affect the mechanical properties of the resulting ceramic composites.

The studies of the micromechanical internal residual stresses in single phase anisotropic polycrystalline materials and in multiphase composites have been ongoing for several decades. Numerous models have been proposed; however, among those various models, modifications of the Eshelby method[22-25] appear to be the most promising. This is because the Eshelby approach can exactly solve the stress field of an anisotropic single crystal grain or second phase inclusion. Using extensions or modifications of the Eshelby method and its matrix forms, the following related problems can be directly addressed:[15]

(i) stresses within an anisotropic single crystal grain or second phase inclusion (whisker),
(ii) the stresses at the interface between an inclusion and the matrix,
(iii) the average residual stress within the matrix,
(iv) the effect or role of the geometry of the inclusion,
(v) the effect of the volume fraction of inclusions or their concentration, and
(vi) the change of the stresses within the inclusion and matrix by applied external stresses.

Figure 1 schematically illustrates an ellipsoidal inclusion which is situated within a composite matrix. The thermal expansions and the elastic properties of the inclusion are anisotropic, while those of the matrix will be considered to be isotropic for the purposes of the calculations. The descriptive geometric parameters of the ellipsoidal inclusion are defined as L and d, where L is specified as parallel to the X_3 axis of the inclusion and d coincides with the X_1 and X_2 axes. If the (L/d) ratio of this ellipsoidal inclusion is equal to unity, then the ellipsoidal inclusion is a spherical grain. For an (L/d) ratio much less than one, the inclusion is a flat tabular plate, and when the (L/d) ratio is much greater than unity the inclusion approximates a whisker. Those three special geometric shapes of the inclusion are also illustrated in Fig. 1. The angle ψ in Fig. 1 is the angle between the X_1 axis and the direction of interest. Two locations in the matrix just outside of the inclusion are of special interest. One is at the

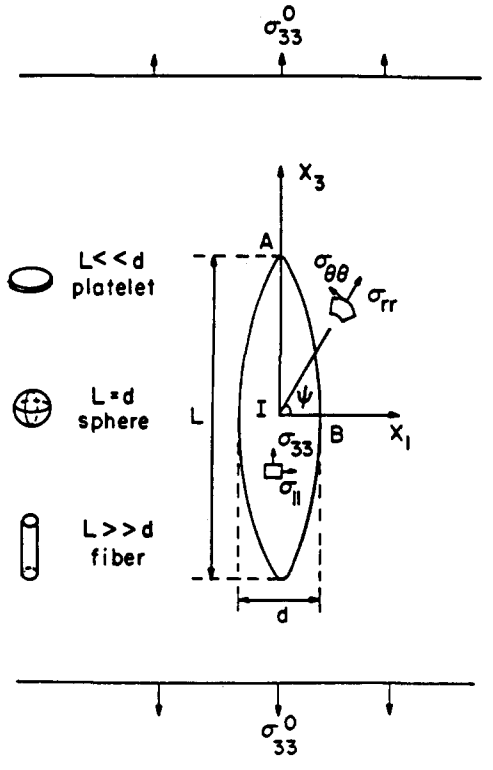

Fig. 1. Schematic of an ellipsoidal inclusion in a ceramic matrix and the stresses of interest.

equator of the inclusion, $\psi = 0°$, as denoted by point B and the other is at the pole of the inclusion, $\psi = 90°$, as denoted by point A.

Details of the mathematical formulation of the micromechanical stress calculations can be found in several references[15,23–25] and are presented here only in their final matrix form. To determine the internal stresses it is necessary to solve for the eigenstrain, ε_{ij}^*, which is generated by the thermal expansion and elastic moduli differences between the anisotropic single crystal reinforcing inclusion and the isotropic polycrystalline matrix. The eigenstrain of the inclusion can be expressed as[15]

$$[\langle C^D\rangle\langle S\rangle + \langle C^M\rangle - V_f\langle C^D\rangle\langle\bar{S}\rangle]\langle\varepsilon^*\rangle = \langle C^I\rangle\langle\varepsilon^T\rangle - \langle C^D\rangle\langle\varepsilon^0\rangle \quad (1)$$

where the $\langle C^I\rangle$, $\langle C^M\rangle$ and $\langle C^D\rangle$ are each 6×6 matrices of the elastic stiffnesses for the inclusion, the matrix, and the difference between the inclusion and the matrix, respectively. The $\langle S\rangle$ and $\langle\bar{S}\rangle$ are 6×6 matrices of the Eshelby tensor and the average Eshelby tensor, respectively. These are directly related to the geometry of the inclusion and the elastic properties of the matrix. The V_f is the volume fraction of the inclusion. The $\langle\varepsilon^0\rangle$, $\langle\varepsilon^T\rangle$ and $\langle\varepsilon^*\rangle$ are each 6×1 matrices of the applied strain, the thermal strain and the eigenstrain, respectively. The ε_{ij}^0 and ε_{ij}^T are given by

$$\varepsilon_{ij}^0 = (C_{ijkl}^M)^{-1}\sigma^0 \quad (2a)$$

and

$$\varepsilon_{ij}^T = (\alpha_{ij}^I - \alpha^M)\,\Delta T \quad (2b)$$

where the $(C_{ijkl}^M)^{-1}$ are the elastic compliances of the matrix. The σ_{ij}^0 is the applied stress and the α_{ij}^I and α^M, respectively, are the thermal expansions of the inclusion and matrix. The ΔT is the temperature difference. Equation (1) is a very general equation that can be considered to be one of the basic equations for the microstructural design of ceramic matrix composites on a mechanics basis.

The stresses inside of the anisotropic inclusion are then

$$\langle\sigma^{in}\rangle = \langle\sigma^0\rangle + \langle C^M\rangle[\langle S\rangle - \langle I\rangle - V_f\langle\bar{S}\rangle]\langle\varepsilon^*\rangle \quad (3)$$

while the average stress in the ceramic matrix is determined from

$$\langle\sigma^M\rangle = \langle\sigma^0\rangle - V_f\langle C^M\rangle\langle\bar{S}\rangle\langle\varepsilon^*\rangle \quad (4)$$

The stresses just outside of the inclusion, in the matrix, are expressed by

$$\langle\sigma^{out}\rangle = \langle\sigma^{in}\rangle - \langle C^M\rangle\langle B\rangle\langle C^M\rangle\langle\varepsilon^*\rangle + \langle C^M\rangle\langle\varepsilon^*\rangle \quad (5)$$

where $\langle I\rangle$ is a 6×6 identity matrix and $\langle B\rangle$ is a 6×6 matrix related to the elastic constants of the matrix and the unit vector outward from the inclusion.[15]

From the above equations it is apparent that the eigenstrain, ε_{ij}^*, is directly related to the internal micromechanical stresses. The eigenstrain and thus the stresses are influenced by the following four parameters: (i) the matrix-inclusion thermal expansion difference, $\Delta\alpha$, (ii) their elastic moduli difference, ΔE, (iii) the geometry of the inclusion, or its aspect ratio, (L/d), and (iv) the volume fraction of the inclusion, V_f. The relationships between the eigenstrain and those four factors are clearly specified through the terms of eqn (1). The first and second terms on the right-hand side of eqn (1), respectively, indicate the effects of $\Delta\alpha$ and ΔE on the stresses. On the left-hand side of eqn (1), the $\langle S\rangle$ and V_f, respectively, indicate the effects of the inclusion geometry and the effects of the concentration of the inclusions. The effects of those four parameters on the internal stresses within Al_2O_3 (sapphire whisker or polycrystalline alumina fiber) reinforced ceramic (mullite and garnet) matrix composites are addressed in Section 3.

Although eqns (1)–(5) appear to be relatively complicated, they have been successfully applied to the composite of SiC whiskers in a polycrystalline alumina matrix by Li and Bradt.[15] The theoretical

calculations based on eqns (1)–(5) are in excellent agreement with the experimental X-ray measurements of Predecki and co-workers[11,13] for the same composite as the magnitudes of the stresses are nearly identical for the theoretical calculations and the experimental measurements. However, more importantly the agreement of the theoretical and experimental results substantiates the necessary assumptions of the calculations, namely that the micromechanical stresses in the whiskers will be highly anisotropic, but those in the matrix are essentially isotropic. Majumdar *et al.*[12] and Tome *et al.*[14] have employed neutron diffraction techniques to determine residual stresses within a similar SiC/Al_2O_3 composite and their results also confirm the theoretical calculations using eqns (1)–(5). Three independent experimental studies have confirmed the Li and Bradt theoretical calculations for SiC/Al_2O_3 composites, based on the anisotropic thermoelastic properties of the whiskers.

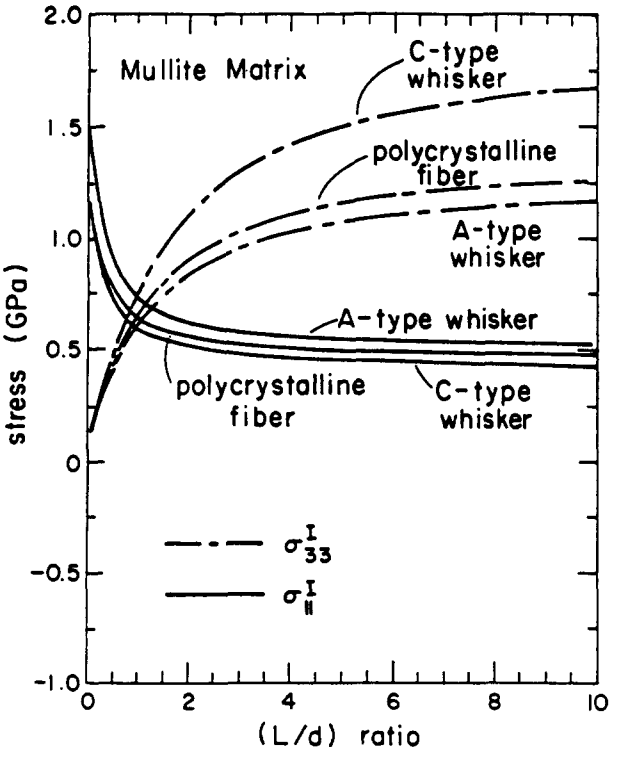

Fig. 2. Stress within a single Al_2O_3 reinforcing inclusion ($V_f = 0{\cdot}0$) as a function of the (L/d) ratio for a mullite matrix composite (all three types of Al_2O_3 are presented).

3 The Micromechanical Stresses in Al_2O_3 Reinforced Composites

By applying eqns (1)–(5) the micromechanical stresses within Al_2O_3 (both sapphire whisker and polycrystalline fiber) reinforced polycrystalline mullite and garnet matrix composites have been calculated. The stresses which are of primary interest are those within the Al_2O_3 reinforcing phase (inclusion), σ^I_{ij}, the stresses just outside of the inclusion, $\sigma^{(out)}_{ij}$, and the average stress in the matrix, σ^M_{ij}. Since $\sigma^{(out)}_{ij}$ are dependent on the angle, ψ, and will have their maximum and/or minimum values at either the A or B points, the stresses just outside of the inclusion can be simply expressed by those extreme values as σ^A_{ij}, and σ^B_{ij}. For random, three-dimensionally oriented inclusions the average stresses in the matrix are the same in all directions as $\sigma^M_{ij} = \sigma^M$.

Assuming a ΔT value of 1000°C, Fig. 2 illustrates the stresses σ^I_{11} and σ^I_{33} within the three different types of Al_2O_3 reinforced structures as a function of their (L/d) ratio for a single inclusion within a mullite matrix composite. The ΔT of 1000°C has been assumed as it is both a logical level for a cooling differential from normal composite processing and also a convenient magnitude for the calculations. Because the thermal expansions of alumina are higher than those of mullite, the stresses within the inclusions will be tensile. The tensile stress, σ^I_{33} in the C-type single crystal whisker is the highest, because the thermal expansion, $\alpha_{\langle 0001\rangle}$, is the largest. The σ^I_{33} for the A-type whisker is the lowest. The polycrystalline alumina fiber stress is intermediate to the two single crystal sapphire orientations. It is important to realise that all of the stresses are dependent on the (L/d) ratios of the reinforcing phase. As the (L/d) ratio increases, the σ^I_{33} also increases while σ^I_{11} decreases. When the geometry of the reinforcing inclusion is a whisker or a fiber with the (L/d) ratio equal to or larger than 10, then the longitudinal tensile stresses are more than 1 GPa. Tensile stresses of this magnitude can easily fracture the sapphire whiskers, or the alumina fibers and generate microcracks within those reinforcing phases. Fractured fibers and whiskers have been observed in Al_2O_3–mullite composites and have been reported by Mah *et al.*[9]

Figure 3 illustrates the stresses within an individual alumina inclusion in a polycrystalline garnet matrix. Since the thermal expansion of garnet is quite similar to those for alumina, the magnitudes of the residual stresses are much lower than for the mullite matrix. For the A-type sapphire whisker and the polycrystalline alumina fiber reinforced garnet matrix composites the stresses within the reinforcing inclusions are actually compressive because $\alpha_{\langle 2\bar{1}\bar{1}0\rangle}$ and $\alpha_{\langle poly\rangle}$ are both less than the thermal expansion of garnet. However, for a C-type sapphire whisker reinforced garnet matrix composite, the σ^I_{33} is in

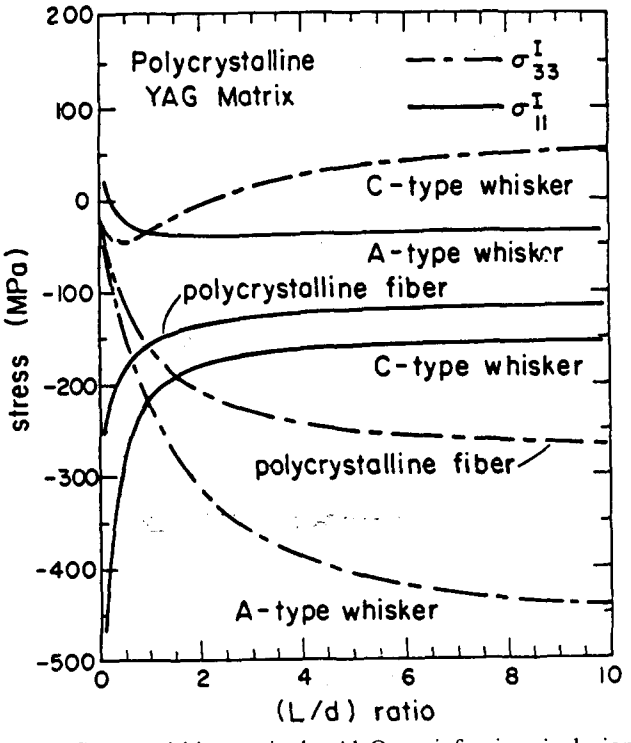

Fig. 3. Stress within a single Al_2O_3 reinforcing inclusion ($V_f = 0{\cdot}0$) as a function of the (L/d) ratio for a garnet matrix composite (all three types of Al_2O_3 are presented).

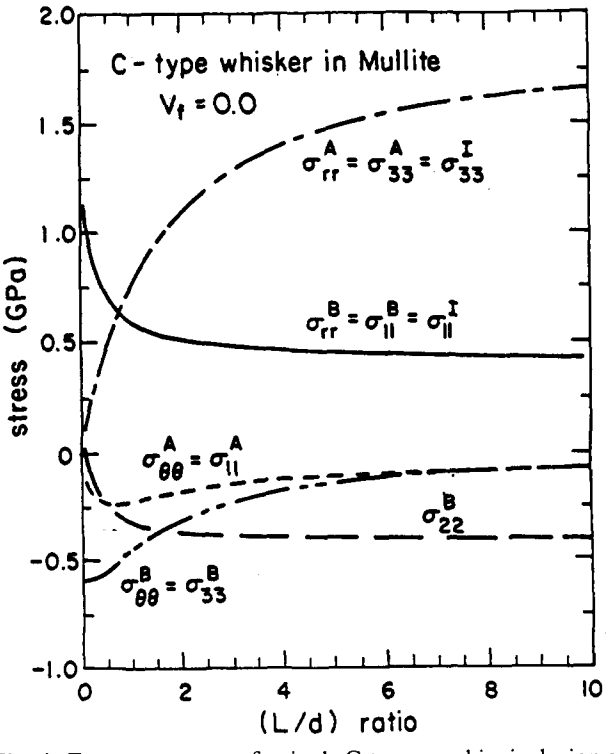

Fig. 4. Extreme stresses of a single C-type sapphire inclusion as a function of (L/d) ratio in a mullite matrix composite.

tension for the $\alpha_{\langle 0001\rangle}$ is higher than the $\alpha_{\langle poly\rangle}$ of garnet. Similar to the mullite matrix composite the magnitudes of the residual stresses in the garnet matrix are also highly dependent on the (L/d) ratio of the reinforcing inclusion. For example, the σ^I_{33} of the A-type whisker increases in compression from 220 MPa at an (L/d) = 1 to 450 MPa at an (L/d) = 10. From Fig. 3 it is evident that it may be difficult for microcracking to occur within the Al_2O_3 reinforcing phase for polycrystalline garnet matrix composites, except perhaps for the case of reinforcement by the C-type sapphire whiskers which are in a state of tensile stress after cooling.

The stresses just outside of the inclusion, at the interface were also calculated for both the mullite and garnet matrix composites. Figure 4 illustrates these stresses for C-type sapphire whiskers in a mullite matrix composite. The radial stresses, $\sigma^A_{rr} = \sigma^A_{33}$ and $\sigma^B_{rr} = \sigma^B_{11}$ are tensile and are equal to the stresses within the inclusion, σ^I_{33} and σ^I_{11}, respectively. The tangential stresses are all compressive and vary with the (L/d) ratio. When the inclusion is a whisker with an (L/d) equal to 10, then σ^A_{11} and σ^B_{33} are essentially zero and σ^B_{22} is about 400 MPa, but in compression. Figure 4 illustrates that of all the stresses, it is the σ^I_{33} which has the maximum value of about 1·6 GPa in tension. This stress level is significant and may be expected to cause fracture of some of the C-type sapphire whiskers within a polycrystalline mullite matrix composite. Figure 5 presents results for polycrystalline alumina fiber reinforced garnet matrix composites. The radial stresses are in compression, although the tangential stresses are tensile. Since the levels of those stresses

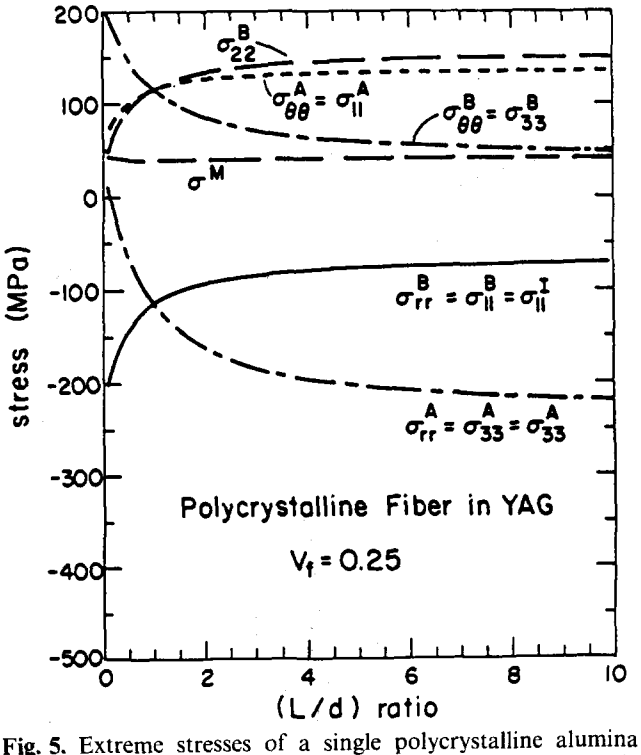

Fig. 5. Extreme stresses of a single polycrystalline alumina inclusion as a function of (L/d) ratio in a garnet matrix composite.

Table 2. Summary of the internal stresses within sapphire whisker and polycrystalline alumina fiber reinforced ceramic matrix composites

	$\sigma^{I}_{11}(MPa)$			$\sigma^{I}_{33}(MPa)$			$\sigma^{M}(MPa)$		
	L/d			*L/d*			*L/d*		
	0·1	*1·0*	*10·0*	*0·1*	*1·0*	*10·0*	*0·1*	*1·0*	*10·0*
$V_f = 0{\cdot}0$ (A single whisker or fiber in an infinite matrix)									
Mullite matrix									
Fiber-poly	+1 179[a]	+649	+467	+125	+649	+1 250	—	—	—
A-type whisker	+1 483	+742	+513	+121	+601	+1 160	—	—	—
C-type whisker	+1 131	+601	+417	+129	+742	+1 662	—	—	—
YAG matrix									
Fiber-poly	−256[b]	−159	−117	−32	−158	−269	—	—	—
A-type whisker	+21	−37	−38	−35	−221	−445	—	—	—
C-type whisker	−468	−221	−157	−25	−37	+50	—	—	—
$V_f = 0{\cdot}15$									
Mullite matrix									
Fiber-poly	+1 019	+537	+347	+2	+537	+1 106	−120	−95	−106
A-type whisker	+1 314	+632	+399	−13	+489	+1 017	−130	−95	−102
C-type whisker	+971	+489	+280	+10	+631	+1 501	−115	−95	−121
YAG matrix									
Fiber-poly	−224	−132	−90	−5	−132	−239	+27	+23	+25
A-type whisker	+43	−10	−4	−17	−194	−405	+18	+23	+31
C-type whisker	−409	−194	−142	+23	−10	+66	+47	+23	+13
$V_f = 0{\cdot}25$									
Mullite matrix									
Fiber-poly	+918	+466	+271	−77	+466	+1 015	−195	−155	−173
A-type whisker	+1 207	+561	+326	−97	+417	+926	−211	−155	−167
C-type whisker	+872	+417	+193	−64	+561	+1 398	−187	−155	−198
YAG matrix									
Fiber-poly	−203	−115	−73	+13	−115	−219	+44	+38	+41
A-type whisker	+57	+7	+18	−5	−176	−380	+30	+39	+51
C-type whisker	−372	−177	−133	+54	+7	+76	+77	+39	+21

[a] +—Tensile.
[b] −—Compressive.

are low, less than 300 MPa, the fracture or microcracking of the fibers and matrix will be much more difficult for a garnet matrix than a mullite one.

The effects of the volume fractions of the reinforcing phases on the magnitudes of the internal stresses for these different composites are illustrated through the summary in Table 2. Figures 6 and 7 illustrate C-type sapphire whisker reinforced mullite matrix and alumina fiber reinforced garnet matrix composites, respectively, for a V_f equal to 0·25 in contrast to the case for only a single inclusion in the previous figures. The magnitudes of the residual stresses within the individual reinforcing sapphire whiskers and alumina fibers are decreased with an increased volume fraction, while those within the matrix just outside of the inclusion are increased, as expected. The average stress inside the ceramic matrix increases from essentially zero for a single inclusion in an infinite matrix to −200 MPa in compression for the mullite matrix and 50 MPa in tension for the garnet matrix when the V_f is equal to 0·25. The average stresses within the ceramic matrices are not as highly dependent on the (*L/d*) ratio of the reinforcing phase as on the volume fraction of that phase.

Table 2 and Fig. 6 suggest that for the mullite matrix composite, even though the matrix appears to be enhanced by a 200 MPa compressive stress, the mechanical properties of those composites may not be significantly improved. The reason for suggesting this is that the very high tensile stresses within the reinforcing phase may easily result in its fracture during cooling from the processing temperature. As previously noted, Mah *et al.* have actually reported the observation of whisker fractures.[9] In contrast, the mechanical properties are more likely to be improved for a garnet matrix composite, especially those for A-type sapphire whisker reinforced garnet composites. This is because the high compressive stresses within the A-type sapphire whiskers may

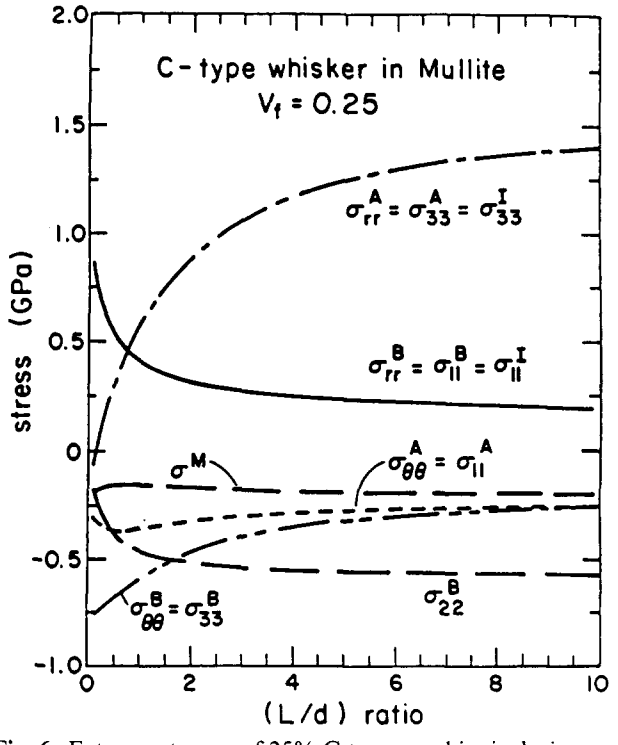

Fig. 6. Extreme stresses of 25% C-type sapphire inclusion as a function of (L/d) ratio in a mullite matrix composite.

inhibit crack propagation and promote whisker bridging of crack faces in the following wake region, once fracture initiates. One might speculate that strongly rising R-curve behavior will be observed for this composite similar to the SiC whisker-reinforced Al_2O_3 which has a comparable stress state.[15]

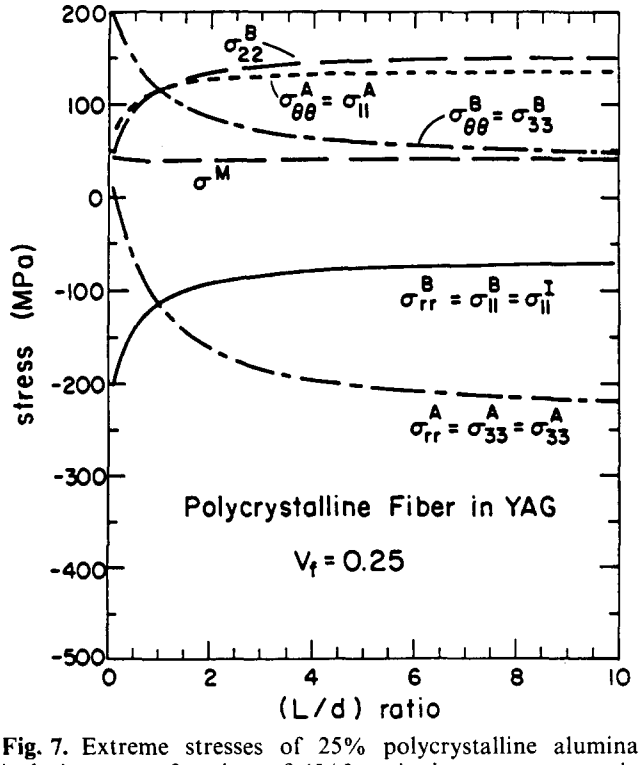

Fig. 7. Extreme stresses of 25% polycrystalline alumina inclusion as a function of (L/d) ratio in a garnet matrix composite.

4 Effect of Applied Stresses

Changes in the internal micromechanical stresses may be expected whenever a load is applied to these composites. A particular case of interest is that of an externally applied uniaxial stress, σ^0_{33}, applied to each of these composites. The stress changes can be calculated based on the assumption that the residual thermal stresses are not relieved by any microcracking during cooling from the processing temperatures or during loading. Figure 8 illustrates these stress changes as the difference, $\Delta\sigma$, between the actual internal stress, σ_{33}, and an applied external stress expressed as σ^0_{33} as a function of the applied external stress for C-type sapphire whisker in a mullite matrix composite and also for the isotropic alumina fiber in a garnet matrix composite. The (L/d) ratio is assumed to equal to 10 and the V_f equal to 0·25 for these calculations. Since the elastic moduli of mullite and garnet are both less than the modulus of alumina, the $\Delta\sigma$ increases significantly within the alumina reinforcing phase. This clearly illustrates that the high elastic modulus reinforcing phase will sustain more of the applied load than the lower elastic modulus matrix. As the stresses within the mullite and garnet matrices only change slightly, it indicates that small amounts of reinforcing phase will not be expected to significantly influence the overall stresses within the matrix.

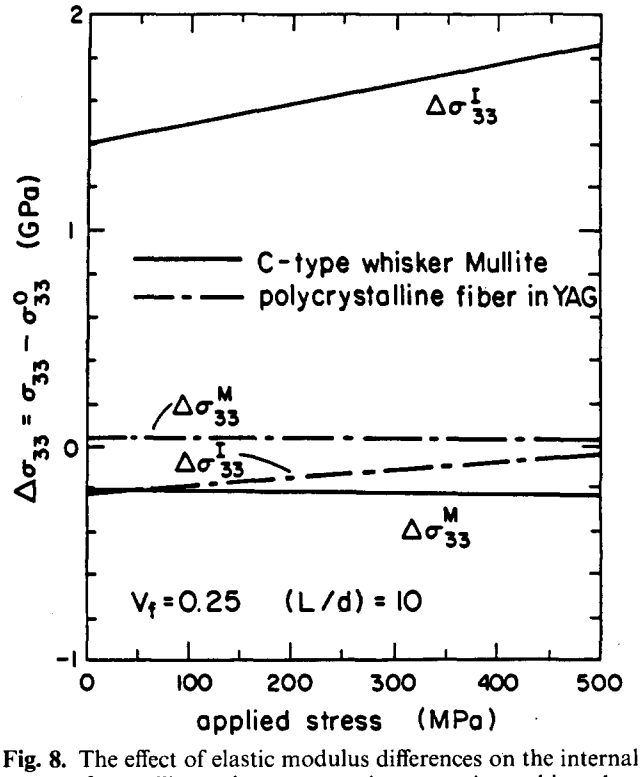

Fig. 8. The effect of elastic modulus differences on the internal stresses for mullite and garnet matrix composites subjected to applied external stresses.

It is evident from both the magnitudes and distributions that these internal micromechanical stresses may assume very important roles in the strengths and toughnesses of ceramic whisker or fiber reinforced polycrystalline ceramic matrix composite materials. From the chemical stability point of view, both mullite and garnet appear to be very promising candidate materials for alumina whisker or fiber reinforced composites, as has been discussed in detail by Mah *et al.*[9] However, the results of the residual stress calculations in this study suggest that the mechanical properties of those two ceramic matrix composites will probably be quite different. The reason for this is the significantly different thermoelastic micromechanical stresses which are generated during cooling from processing temperatures. For the mullite matrix composites the very high residual tensile stresses may be expected to be detrimental to the integrity of the Al_2O_3 reinforcing phases. However, for the garnet matrix composites, especially for those reinforced by A-type sapphire whiskers, compressive stresses will be generated within the whiskers during cooling from processing. Therefore, to design a promising composite material, the residual micromechanical internal stresses must be considered as well as the chemical and thermodynamic stability criteria.

5 Summary and Conclusions

Micromechanical residual stresses resulting from thermoelastic property differences were calculated for the reinforcing phases of two orientations of anisotropic sapphire single crystal whiskers and for isotropic polycrystalline alumina fibers in polycrystalline mullite and garnet ceramic matrix composites. These internal stresses may vary from the MPa to the GPa range in tension or compression, depending on the thermal expansion and elastic modulus differences as well as the inclusion geometry and volume fraction of the reinforcing phase. The results indicate that even though the thermodynamic stability of sapphire whiskers in a mullite matrix is appealing, the residual stress situation is highly unsatisfactory. Large tensile stresses which are conducive to internal fractures are present in the whiskers of that composite system. In contrast, a garnet matrix has a coefficient of thermal expansion which lies between the principal axial α_{11} and α_{33} values of sapphire and yields a much more favourable internal residual stress distribution. Alumina fibers with a polycrystalline structure are intermediate to the C-type and A-type sapphire whiskers. All alumina reinforcements, however, will carry a large fraction of any externally applied loads as the elastic moduli of alumina are much greater than those of mullite or garnet.

References

1. Becker, P. F. & Wei, G. C., Toughening behavior in SiC-whisker reinforced alumina. *J. Amer. Ceram. Soc.*, **67** (1984) C267–9.
2. Jenkins, M. G., Kobayashi, A. S., White, K. W. & Bradt, R. C., Crack initiation and arrest in a SiC whisker/Al_2O_3 matrix composite. *J. Amer. Ceram. Soc.*, **70** (1987) 393–5.
3. Homeny, J., Vaughn, W. L. & Ferber, M. K., Processing and mechanical properties of SiC–whisker–Al_2O_3-matrix composites, *Amer. Ceram. Soc. Bull.*, **66** (1987) 333–8.
4. Shalek, P. D., Petrovic, J. J. Hurley, G. F. & Gac, F. D., Hot-pressed SiC whisker/Si_3N_4 matrix composites. *Amer. Ceram. Soc. Bull.*, **65** (1986) 351–66.
5. Lundberg, R., Kahlman, L., Pome, R., Carlsson, R. & Warren R., SiC-whisker-reinforced Si_3N_4 composites. *Amer. Ceram. Soc. Bull.*, **66** (1987) 330–3.
6. Singh, J. P., Goretta, K. C., Kupperman, D. S., Routbort, J. L. & Rhodes, J. F., Fracture toughness and strength of SiC-whisker-reinforced Si_3N_4 composites. *Adv. Ceram. Mater.*, **3** (1988) 357–60.
7. Singh, R. N. & Gaddipati, A. R., Mechanical properties of a uniaxially reinforced mullite-silicon carbide composite. *J. Amer. Ceram. Soc.*, **71** (1988) C100–3.
8. Klug, F. J., Prochazka, S. & Doremus, R. H., Al_2O_3–SiO_2 phase diagram in the mullite region. *J. Amer. Ceram. Soc.*, **70** (1987) 750–9.
9. Mah, T., Mendiratta, M. G. & Boothe, L. A., High temperature stability of refractory oxide–oxide composites. Technical report AFWAL-TR-88-4015, Air Force Wright Aeronautical Laboratory, Dayton, OH, 1988.
10. Li, Z. & Bradt, R. C., Thermoelastic anisotropy in SiC, residual stresses in monolithic SiC ceramics and SiC whisker reinforced composites. *Mater. Sci. Forum*, **34–36** (1988) 551–23.
11. Predecki, P., Abuhasan, A. & Barrett, C. S., Residual stress determination in Al_2O_3/SiC (whisker) composites by X-ray diffraction. *Adv. X-Ray Anal.*, **31** (1988) 231–243.
12. Majumdar, S., Kupperman, D. & Singh, J., Determination of residual thermal stresses in a SiC–Al_2O_3 composite using neutron diffraction. *J. Amer. Ceram. Soc.*, **71** (1988) 858–63.
13. Abuhasan, A., Balasingh, C. & Predecki, P., Residual stresses in alumina/silicon carbide (whisker) composites by X-ray diffraction. *J. Amer. Ceram. Soc.*, **73** (1990) 2474–84.
14. Tome, C. N., Bertinetti, M. A. & MacEwen, S. R., Correlation between neutron diffraction measurements and thermal stresses in a silicon carbide/alumina composite. *J. Amer. Ceram. Soc.*, **73** (1990) 3428–32.
15. Li, Z. & Bradt, R. C., Micromechanical stresses in SiC-reinforced Al_2O_3 composites. *J. Amer. Ceram. Soc.*, **72** (1989) 70–7.
16. Tefft, W. E., Elastic constants of synthetic crystal corundum. *J. Res. Nat. Bur. Stand.*, **70A** (1960) 227–80.
17. Eckert, L. J. & Bradt, R. C., Thermal expansion anisotropy of corundum—type structure single cation oxides. In *Thermal Expansion 8*, ed. T. Hahn. Plenum Pub. Co., New York, USA, 1983, pp. 58–68.
18. Salem, J. A., Li, Z. & Bradt, R. C., Thermal expansion and elastic anisotropy in single crystal Al_2O_3 and SiC whiskers. In *Proc. of Symp. on Advances in Composite Materials and Structures*, ed. S. S. Wang. ASME, Fairfield, NJ, USA, 1989, pp. 37–43.
19. Mazdiyasni, K. S. & Brown, L. M., Synthesis and

mechanical properties of stoichiometric aluminum silicate (mullite). *J. Amer. Ceram. Soc.*, **55** (1972) 548–52.
20. Gupta, T. K. & Velentich, J., Thermal expansion of yttrium aluminum garnet. *J. Amer. Ceram. Soc.*, **54** (1971) 355–6.
21. Spencer, E. G., Denton, R. T., Bateman, T. B., Snow, W. B. & Van Uitert, L. G., Microwave elastic properties of nonmagnetic garnets. *J. Appl. Phys.*, **34** (1963) 2059–3060.
22. Eshelby, J. D., The determination of the elastic field of an ellipsoidal inclusion, and related problems. *Proc. Royal Soc. London, Ser. A*, **241** (1967) 376–96.
23. Mura, T., *Micromechanics of Defects in Solid.* Martinus Nijhoff Publishers, The Hague, The Netherlands, 1982, pp. 66–75.
24. Khachaturyan, A. G., *Theory of Structural Transformations in Solids.* John Wiley & Sons, New York, USA, 1983, pp. 226–40.
25. Taya, M., On stiffness and strength of an aligned short fiber reinforced composite containing penny-shaped crack in the matrix. *J. Comp. Mater.*, **15** (1981) 198–210.